Quantum Electronics **38** (4) 391 – 400 (2008)

LASER SPECTROSCOPY

PACS numbers: 42.62.Eh; 42.62.Fi; 42.55.Px
DOI: 10.1070/QE2008v038n04ABEH013680

Spectral parameters of reference-cavity-stabilised lasers

A.N. Matveev, N.N. Kolachevsky, J. Alnis, T.W. Hänsch

Abstract. **Spectral characteristics of laser systems used for precision two-photon spectroscopy of the 1s – 2s transition in the hydrogen atom are analysed. The spectral properties of radiation from a 972-nm external-cavity semiconductor laser stabilised by external monolithic cavities of different configurations are considered in detail. The classical cavity scheme with a horizontal axis and a new scheme with a vertical axis, which is weakly sensitive to vibrations, are considered. The emission spectrum of a stabilised laser exhibits a narrow central peak and a pedestal caused by the residual phase noise. The semiconductor laser stabilised with respect to the vertical-axis cavity emits the line of width less than 0.45 Hz, which contains ~99 % of the total output power. The transformation of the emission spectrum upon frequency doubling in nonlinear crystals is investigated. The laser system developed in the study provides the narrowing of the recorded 1s – 2s transition line in the hydrogen atom down to 2 kHz at 121 nm.**

Keywords: *ultrahigh-resolution spectroscopy, stabilisation by the reference cavity by the Pound – Drever – Hall method.*

1. Introduction

Considerable recent progress achieved in high-resolution laser spectroscopy is related to the possibility of observing narrow (~10 Hz) atomic transition lines in the visible and UV spectral ranges [1 – 3]. The spectroscopy of such narrow resonances requires highly stable lasers emitting very narrow lines of width considerably smaller than the transition linewidth. This stimulated the development of methods for stabilising laser systems to achieve subhertz spectral linewidths for lasers emitting lines of width of a few tens of megahertz in the unstabilised regime and tunable within tens of nanometres. Such a considerable laser line narrowing is achieved in most cases by using the electronic frequency stabilisation with respect to the transmission peak of a high-Q monolithic Fabry – Perot cavity. This method provides the narrowing of the laser line to the width that is almost completely determined only by vibrations and thermal fluctuations of the reference cavity [4].

We studied the 1s – 2s two-photon transition in the hydrogen atom with the natural linewidth equal to 1.3 Hz. The transition was excited in a cold atomic beam by a stabilised laser system at 243 nm (see, for example, [5]). At present laser systems of two types are used for this purpose: (i) a Coumarin 102 dye laser emitting radiation at 486 nm, which is then frequency-doubled in a barium beta borate crystal [5, 6] or (ii) a semiconductor laser emitting radiation at 972 nm, which is amplified in a horn-type amplifier and then is converted to the 243-nm radiation after two successive frequency doublings [7]. Unlike other laser systems used for the spectroscopy of laser-cooled localised atoms and ions [1 – 3], the interaction time with hydrogen atoms in the laser beam in the laser systems under study is ~1 ms, which requires the use of high-power laser fields providing high Rabi frequencies (~1 kHz) for a weak two-photon transition. In addition, successive frequency doublings impose rigid requirements on the fundamental radiation spectrum of the laser. Note that from the point of view of the spectrum conversion, two-photon absorption is equivalent to the second harmonic generation [8].

In this paper, we consider two 972-nm reference cavities that we developed to stabilise the frequency of a semiconductor laser. The cavities are assembled by using a new scheme with the vertical axis, which considerably reduces their sensitivity to vibrations and allows the development of compact laser systems with excellent frequency-phase characteristics [9]. We analysed the spectral characteristics of the laser system stabilised with the help of these cavities and compared them with other cavities at our disposal. The transformation of spectral characteristics of radiation of the diode laser system upon frequency doubling in a nonlinear crystal was studied. By using a 972-nm laser stabilised with a vertical-axis cavity, we recorded spectra of the 1s – 2s transition in the hydrogen atom and compared them with spectra recorded earlier by using other laser systems [7].

2. The Pound – Drever – Hall method

The high stability of the laser radiation frequency can be achieved only by the active stabilisation of the laser cavity

A.N. Matveev, N.N. Kolachevsky P.N. Lebedev Physics Institute, Russian Academy of Sciences, Leninsky prosp. 53, 119991 Moscow, Russia; e-mail: amatveev@mpq.mpg.de, kolik@lebedev.ru;
J. Alnis Max Planck Institute of Quantum Optics, Hans-Kopfermann-Str. 1, 85748 Garching, Germany; e-mail: Janis.Alnis@mpq.mpg.de;
T.W. Hänsch Max Planck Institute of Quantum Optics, Hans-Kopfermann-Str. 1, 85748 Garching, Germany; Ludwig-Maximilians University, Geschwister-Scholl-Platz 1, 80539 Munich; e-mail: t.w.haensch@mpq.mpg.de

Received 3 July 2007; revision received 22 November 2007
Kvantovaya Elektronika **38** (4) 391 – 400 (2008)
Translated by M.N. Sapozhnikov

with respect to the external reference cavity well isolated from external perturbations (see, for example, [3, 5, 10]). The laser radiation frequency can be locked to the transmission maximum of the external cavity by different methods, for example, by using optical feedback from the cavity or electronic feedback loops. Lasers used in precision spectroscopy are commonly stabilised by the modulation method proposed by Pound, Drever, and Hall (PDH) [11], which is illustrated schematically in Fig. 1. Laser radiation is modulated by phase with an electrooptical modulator at frequency Ω (usually, tens of megahertz) and is coupled into a stable cavity. The radiation reflected back from the cavity is detected with a photodetector whose output signal is heterodyned in a balance mixer with a radiofrequency signal of the same frequency Ω. After heterodyning, the signal passes through a low-frequency filter and is used as the error signal in a feedback system controlling the laser frequency.

To obtain the error signal in the PDH method, we represent the output signal of the photodetector as a result of the interference of two waves, one of which appears after the propagation of radiation 'stored' in the cavity through the front mirror and the second one appears upon the reflection of radiation incident on the front mirror:

$$S_{\rm pd} \propto \Big\langle |TA_1 \exp[{\rm i}(\omega_0 t + \phi_1)] - RA \exp[{\rm i}(\omega_0 t + \phi + \phi_{\rm mod}\cos\Omega t)]|^2 \Big\rangle = [(TA_1)^2 + (RA)^2 - 2TRAA_1 \cos(\Delta\phi + \phi_{\rm mod}\cos\Omega t)], \quad (1)$$

where T and R are the amplitude transmission and reflection coefficients of mirrors; ω_0 is the radiation frequency; A is the incident wave amplitude; A_1 is the amplitude of the wave incident on the front mirror of the cavity from inside; ϕ and ϕ_1 are the phases of these waves, respectively; $\phi_{\rm mod}$ is the depth of phase modulation of the incident wave; and $\Delta\phi = \phi - \phi_1$ is the phase difference of the two light waves. The angle brackets denote averaging over the photodetector passband. Taking into account only low-frequency spectral components in the heterodyne signal, we obtain the error signal

$$S_{\rm err} = \langle S_{\rm pd} \cos\Omega t \rangle \propto TRAA_1 \phi_{\rm mod} J_0(\phi_{\rm mod}) \sin\Delta\phi, \quad (2)$$

where $J_0(\phi_{\rm mod})$ is the Bessel function the first kind. Because in the case when the laser is preliminarily stabilised by the cavity, the phase difference between radiation and a standing wave is small, the error signal proves to be proportional to the phase difference: $S_{\rm err} \propto \Delta\phi$. One can see from this relation that the stabilisation of the laser with respect to a Fabry–Perot resonator by the PDH method represents in fact the phase locking of laser radiation to the standing wave in the cavity.

To obtain the shape of the error signal, we consider the case when the laser linewidth is much narrower than the width of the transmission peak of the interferometer. In this case, laser radiation excites a standing wave in the cavity whose phase can differ from that of the exciting wave. By neglecting the influence of phase-modulation harmonics on the standing wave, we find the amplitude A_1 and phase difference $\Delta\phi$:

$$A_1 = \frac{ATJ_0(\phi_{\rm mod})}{[1 - 2R^2\cos(2\pi\omega/\omega_{\rm FSR}) + R^4]^{1/2}}, \quad (3)$$

$$\sin\Delta\phi = \frac{R^2}{[1 - 2R^2\cos(2\pi\omega/\omega_{\rm FSR}) + R^4]^{1/2}} \sin\left(\frac{2\pi\omega}{\omega_{\rm FSR}}\right), \quad (4)$$

where $\omega_{\rm FSR} = 2\pi c/(2L)$ is the free spectral range (in frequency) of the cavity; c is the speed of light: and L is the cavity length. This gives the error signal

$$S_{\rm err} = \frac{kA^2T^2R^3\phi_{\rm mod}J_0^2(\phi_{\rm mod})}{1 - 2R^2\cos(2\pi\omega/\omega_{\rm FSR}) + R^4} \sin\left(\frac{2\pi\omega}{\omega_{\rm FSR}}\right). \quad (5)$$

A rigorous mathematical description of the signal shape obtained by the PDH method is presented, for example, in [12]. Figure 2a shows the typical error signal described by expression (5). At the maximum of the cavity transmission, i.e. for $\omega \approx N\omega_{\rm FSR}$, the error signal is $S_{\rm err} \propto \omega - n\omega_{\rm FSR}$, corresponding to expression (2). Note that the shape of the error signal depends considerably on the phase of a reference signal used in heterodyning (Fig. 1). The signal shape presented in Fig. 2 corresponds to the phase shift by $\pi/2$ in a phase shifter.

A more complicated is the case of stabilising the frequency of a laser with the linewidth greatly exceeding the width of the transmission band of the cavity. It is this situation that we are dealing with by stabilising a semiconductor laser emitting the line of width $\sim$1 MHz with respect to a high-Q cavity with the width of the transmission band 5 kHz. In this case, the error signal contains information not only on the laser frequency detuning but also on the

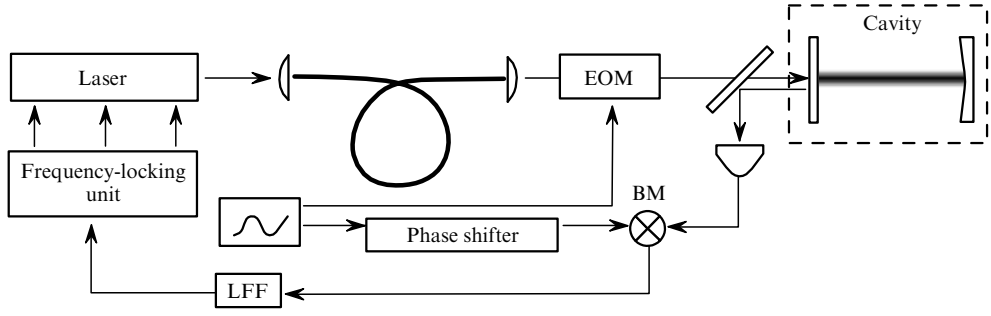

Figure 1. Scheme for laser frequency stabilisation by the Pound–Drever–Hall method: (EOM) electrooptical modulator; (BM) balance mixer; (LFF) low-frequency filter.

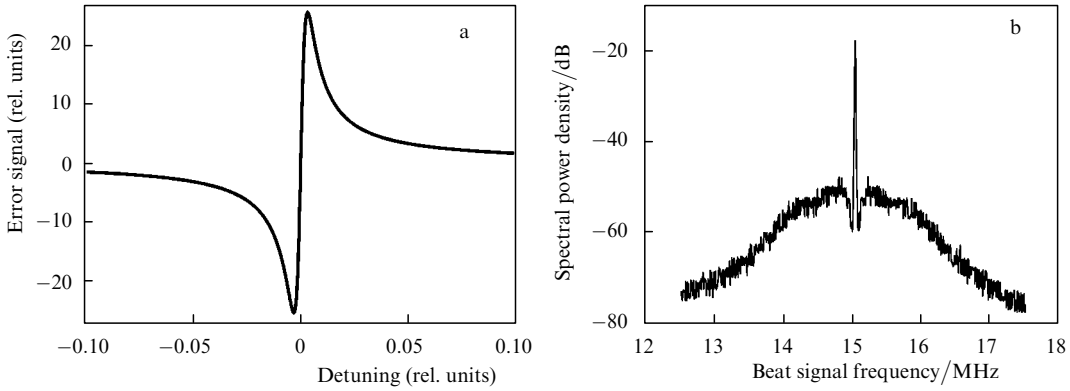

Figure 2. Central part of the error signal obtained by the PGH method by scanning the transmission band of the cavity by narrowband laser radiation (a) and the emission spectrum of the diode laser stabilised with respect to the external stable cavity by the PDH method (b).

rapid phase noise [$S_{\rm err} \propto \Delta\phi(t)$] determining the initial spectral linewidth on the unstabilised laser. It was shown in [11] that the laser linewidth can be efficiently narrowed down in this case as well by using the active stabilisation of the cavity by the PDH method due to the presence of broad dispersion wings of the error signal. In this case, the emission spectrum of the stabilised laser is noticeably transformed and its shape will depend considerably both on the type of the phase noise of the unstabilised laser and feedback loop parameters. For example, the emission spectrum of an electronically stabilised diode laser exhibits a narrow peak (carrier) of width $\sim$1 MHz located on a pedestal of complicated shape (Fig. 2b). Similar spectra were observed in experiments on the phase locking of diode lasers to other radiation sources such as a femtosecond frequency comb [13] or another diode laser [14]. In the case of stabilisation of lasers of other types (for example, dye lasers or Ti : sapphire lasers), the pedestal is less pronounced.

3. Reference cavities

It is known that the distance between the mirrors of the reference cavity almost completely determines the radiation frequency of a stabilised laser. The cavity length depends mainly on mechanical vibrations and thermal fluctuations. To suppress the latter, the cavity body is made of materials with low coefficients of thermal expansion and the cavity temperature is stabilised. Seismic and acoustic vibrations are suppressed by using various active and passive suppression systems. In addition, in recent papers [9, 15] the cavity configuration was selected so that the sensitivity to vibrations (accelerations) was minimised.

We manufactured earlier two 486-nm cavities (denoted by 1 and 2) having the classical horizontal configuration, which were used to stabilise a dye laser [5]. Cavities of length 15 cm with a Q factor of 90 000 are shown schematically in Figs 3a, b. These two cavities differ in the method of their mounting on an optical table: cavity 1 was supported from below by three bearings touching directly the optical table, whereas cavity 2 suspended on long springs. Optical tables on which the cavities were mounted were equipped with active vibration compensation systems (Halcyonics).

To perform the spectroscopic study of the 1s–2s transition in the hydrogen atom by using a semiconductor laser system [7], we constructed two stabilisation systems for 972-nm cavities. These cavities (denoted by 3 and 4) had a length of 7.5 cm and a Q factor of 420000 and were mounted in the vertical configuration (Fig. 3c).

The bodies of all the cavities were made of an ULE (Ultra Low Expansion) glass [16] for which the relative elongation of a sample of length l with temperature t is described by the expression $\delta l/l \approx 10^{-8}(t - t_{\rm c})^2$, where $t_{\rm c}$ is the so-called critical temperature, which lies usually in the range from 0 to 20 °C. The cavities were housed in chambers evacuated to 10^{-8} bar with the help of ion–getter pumps. The temperature of cavities 1, 2, and 3 was stabilised by using identical thermal stabilisation systems consisting of

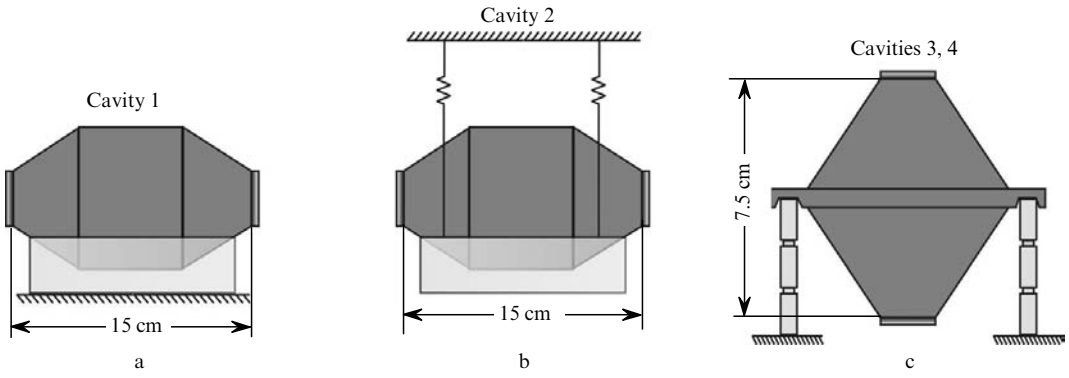

Figure 3. Mountings of cavities used in experiments.

two stages. The external stage maintaining a stable temperature background around the vacuum chamber was based on a six-channel relay scheme. Each channel maintained the temperature of one of the six walls of the box surrounding the chamber at a level several degrees above room temperature with an accuracy of $\sim$100 mK at the sensor location. An advantage of the relay scheme is its rapid response to temperature variations. The internal stabilisation system had a large time constant and maintained the temperature of the vacuum chamber with an accuracy of 1 mK by means of the integrated feedback loop. A disadvantage of this system was that it could not provide the temperature stabilisation with respect to the zero point of the ULE glass ($t = t_c$), which was considerably lower than room temperature in our case (see below).

The system of temperature stabilisation of cavity 4 provided the cooling of the chamber. The cavity body located in the vacuum chamber was surrounded by two aluminium cylinders. Both between the cylinders and between the external cylinder and vacuum chamber, Peltier elements were located which were used to cool cylinders and stabilise their temperature. The temperature stability provided by this system was considerably worse than that ensured by the first system. For example, the temperature stability inside the cylinder could be maintained only with an accuracy of 10 mK.

We measured the critical temperature t_c for our ULE glass sample. By using cavity 3 as a reference cavity and varying the temperature of cavity 4 in the range from 7 to 20 °C, we found $t_c = 12.5$ °C. The cavity body length at this point is minimal and, therefore, the beat frequency between laser fields stabilised with respect to the corresponding transmission maxima of cavities is maximal. Unfortunately, the thermal expansion of a multilayer coating (38 Ta_2O_5 and 38 SiO_2 layers of a total thickness $\sim$5 μm were deposited on each mirror) exceeds the thermal expansion of the cavity body, which imposes strict requirements on the thermal stabilisation system.

The analysis of deformations of the cavity body during its acceleration, for example, in the vertical direction showed that the cavity configuration with the horizontal axis is quite sensitive to vibrations. This is clearly demonstrated by computer simulations performed by using the Autodesk Inverter software package (Fig. 4a). If the cavity is supported from below, acceleration in the vertical direction elongates or compresses the cavity, resulting in a change in the distance between mirrors and, therefore, in a change in the radiation frequency of the stabilised laser. Note that it is possible to fix the cavity at certain points to minimise this effect. However, this requires a very careful individual selection of fixing points for each cavity.

In another approach developed a few years ago (see, for example, [17]), a cavity is suspended by the plane passing through its centre of gravity. Thus, in the case of a vertical-axis cavity shown in Fig. 4b, the vertical acceleration will cause the symmetric deformation of its upper and lower parts, thereby retaining the distance between mirrors with a high accuracy because the decrease in the length of the upper part of the cavity body is compensated by the elongation of its lower part.

In this paper, we compared the spectral characteristics of lasers stabilised with respect to cavities 1, 2, 3, and 4 shown in Fig. 3.

4. Laser systems

We studied two laser systems shown schematically in Fig. 5. The first system – a 486-nm Coumarin 102 dye laser, was stabilised by the PDH method with respect to cavity 1 or 2. In all experiments considered below, stabilisation with respect to cavity 2 was used, the stabilisation parameters remaining invariable. The laser frequency was controlled by means of an intracavity electrooptical modulator (EOM), a mirror on a piezoelectric ceramics and a galvanoplate. The laser radiation was frequency-doubled in a second-harmonic generator (SHG 1) to produce $\sim$20 mW of output power at 243 nm for exciting the 1s–2s transition in the hydrogen atom.

The second laser system was based on a semiconductor laser with an external cavity in Littrow mounting [7]. The laser radiation amplified in a tapered semiconductor amplifier up to 650 mW was frequency-doubled in two stages (SHGs 2 and 3) to produce $\sim$10 mW of output power at 243 nm. The laser was stabilised with respect to cavities 3

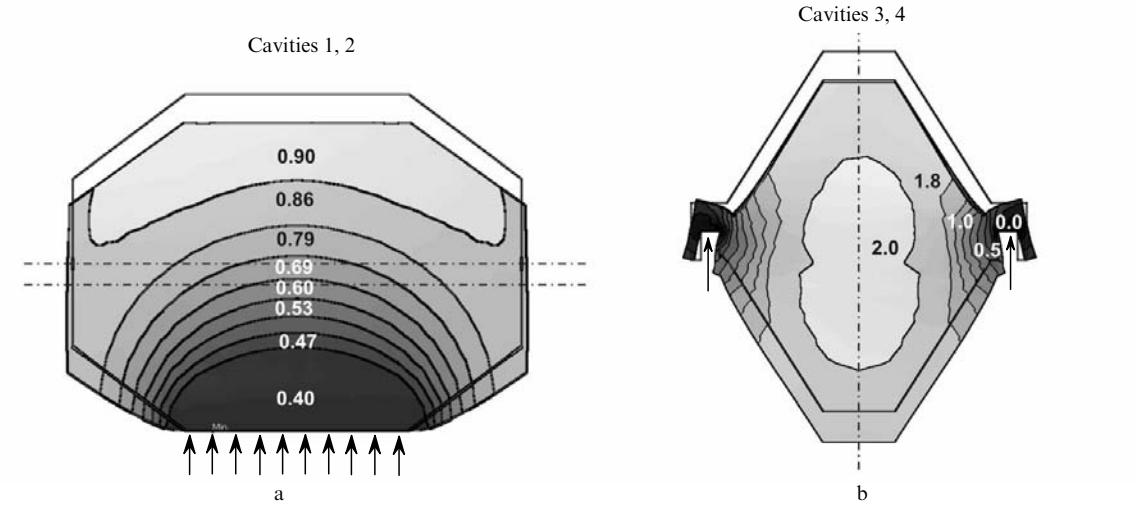

Figure 4. Calculation of the deformation of model cavities under the action of acceleration 1g; cavity sizes are presented in Fig. 3; the numbers are deformation in nanometres.

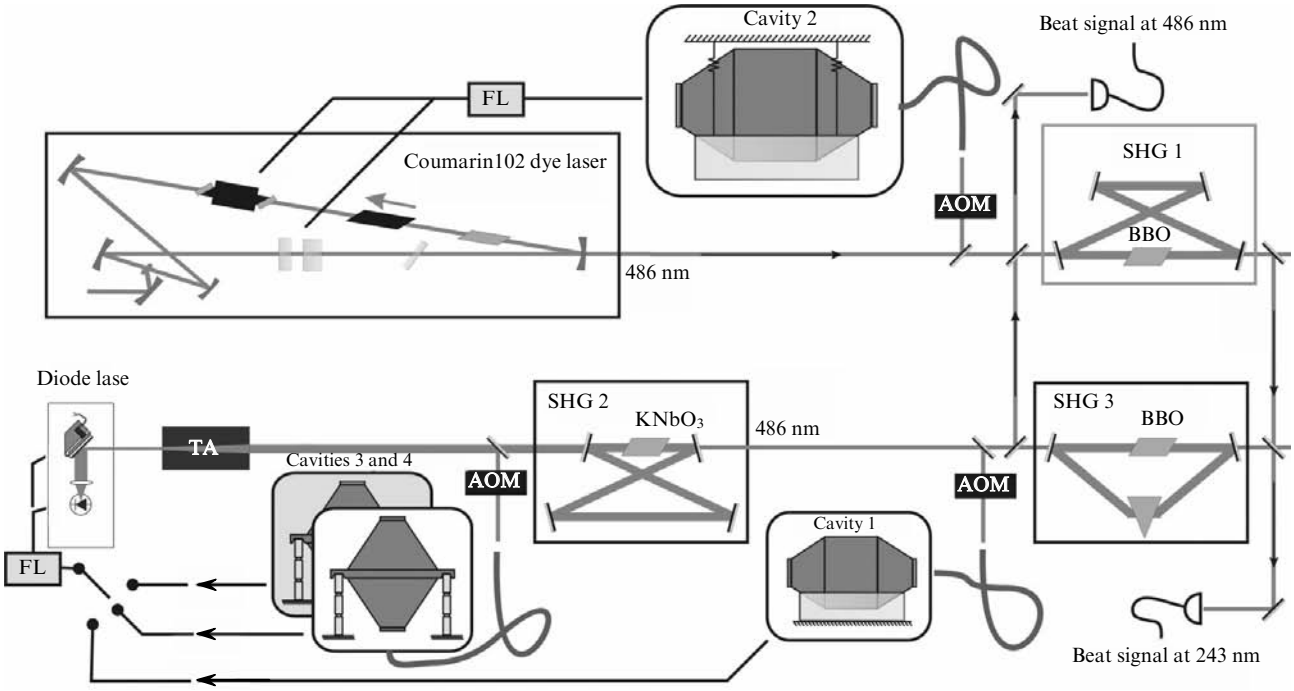

Figure 5. Schemes of laser systems: (AOM) acoustooptic modulator; (SHG 1, 2, 3) second-harmonic generators; (TA) tapered semiconductor amplifier; (FL) feedback loop in the PDH method.

and 4 at a wavelength of 972 nm. It was also possible to stabilise it by cavity 1 by using the 486-nm second-harmonic radiation at the output of SHG 2 (Fig. 5). The laser frequency was controlled by varying the injection current of the diode (proportional fast and integral slow channels) and by rotating a diffraction grating.

Laser radiation was coupled into cavities through single-mode fibres. Because radiation propagating in a fibre acquires additional phase and amplitude noises, we used classical schemes with an acoustooptic modular (AOM) compensating these noises [18].

We studied the spectra of beat signals between radiations from the diode laser system and the dye laser at wavelengths 486 and 243 nm. The dye laser was used as the reference laser, while the parameters of the feedback system of the semiconductor laser were varied. We also performed measurements by using cavities 1, 3, and 4. The spectral characteristics of cavities 3 and 4 were investigated by using the scheme shown in Fig. 6 which was proposed in [19]. Radiation from a diode laser stabilised with respect to cavity 1 passed through AOM 1 and was coupled to cavity 3. The error signal from cavity 4 was fed to the frequency-modulation input of a voltage-controlled oscillator (VCO) which excited AOM 2. In this way the laser radiation frequency was locked to the frequency of the transmission band of cavity 3, while the field frequency at the AOM 2 output proved to be stabilised with respect to the maximum of the transmission band of cavity 4. In the case of independent vibrations of cavities, the phase fluctuations of laser fields in front and behind AOM 2 prove to uncorrelated within the frequency band of the feedback loop controlling the VCO. The spectral width of the beat signal between these fields gives the estimate of the linewidth of a stabilised semiconductor laser with an accuracy to a coefficient ~ 1 depending on the shape of the spectrum.

5. Power fraction in the carrier

We will analyse the emission spectrum of a stabilised diode laser and its transformation upon frequency doubling by using the following model. First of all, we will take into account that the initial emission spectrum of a semiconductor laser is mainly formed due to rapid phase

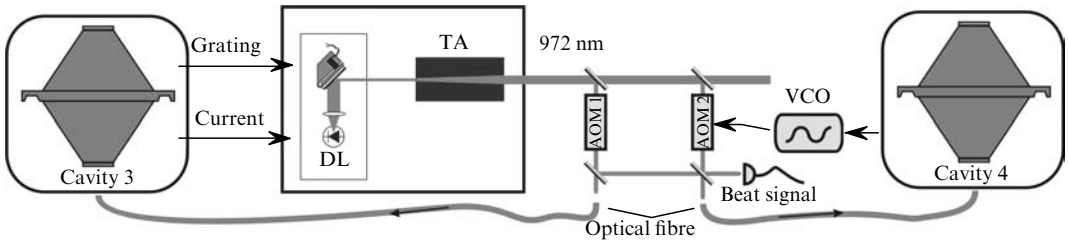

Figure 6. Scheme for measuring the linewidth of the diode laser (DL) stabilised with respect to cavity 3.

fluctuations caused by spontaneous emission events and a change in the carrier density (see, for example, [12]). Let us assume that laser radiation at frequency ω_0 is stabilised in phase with respect to another field with the phase $\phi_0(t)$, which is 'stored' in a high-Q cavity. Because the phase stabilisation of the semiconductor laser is not ideal, the laser radiation field $E(t) = E_0 \cos[\mathrm{i}(\omega_0 t + \phi_0(t) + \phi(t))]$ has the fluctuating phase component $\phi(t)$. Fluctuations $\phi(t)$ are determined by the noises of the laser diode and electronic elements used in the feedback loop, and therefore the characteristic correlation time for these fluctuations is ~ 0.1 μs. The correlation time of the phase noise in the cavity (the decay time of a wave in the cavity) is ~ 100 μs; therefore, we can set $\phi_0(t) = \text{const}$. Let us also assume that the residual phase noise is described by the normal distribution

$$p(\phi) = \frac{1}{\sqrt{2\pi}} \exp\left(-\frac{\phi^2}{2\phi_{\mathrm{rms}}^2} \right),$$

where ϕ_{rms} is the root-mean-square phase deviation appearing due to the incomplete response of the feedback system. Then, the autocorrelation function $R_E(\tau)$ of the laser field will have the form

$$R_E(\tau) = \langle E(t)E(t+\tau) \rangle = \frac{1}{2} \cos(\omega_0 \tau) \langle \cos \Delta\phi(t,\tau) \rangle, \qquad (6)$$

where the angle brackets denote averaging and $\Delta\phi(t,\tau) = \phi(t+\tau) - \phi(t)$. Because the laser-field phase is actively stabilised, we have $\lim_{\tau\to\infty} \cos \Delta\phi(t,\tau) \neq 0$. This means that the Fourier transform of the autocorrelation function (spectral power density of the process) will contain the delta function at the frequency ω_0, which is called the carrier frequency. The power fraction η contained in the carrier is proportional to $\langle \cos \Delta\phi(t, \tau \to \infty) \rangle$. We will calculate this parameter taking into account that the noises of the phase ϕ at such times are not correlated:

$$\eta \propto \int_{-\infty}^{+\infty} \int_{-\infty}^{+\infty} \cos(\phi_2 - \phi_1) p(\phi_1) p(\phi_2) \mathrm{d}\phi_2 \mathrm{d}\phi_1 = \exp(-\phi_{\mathrm{rms}}^2). \qquad (7)$$

Because $\phi_{\mathrm{rms}} = 0$, we have $\eta = 1$, i.e. the field proves to be monochromatic, and we obtain finally $\eta = \exp(-\phi_{\mathrm{rms}}^2)$.

Upon frequency multiplication by n times (n-photon process), the laser field phase is multiplied by η'. Taking this fact into account, we obtain the power fraction

$$\eta' = \eta^{n^2} \qquad (8)$$

contained in the carrier after conversion to the nth harmonic.

If radiation is multiply converted to higher harmonics, the parameter η' becomes critical. A typical example is the so-called frequency chains [12] – many stages of the nonlinear frequency conversion from the radiofrequency to optical range. It was concluded in [20] that the single-stage frequency conversion from the radiofrequency to optical range is impossible due to the 'carrier collapse' caused by the increase in the noise power. Note that the optical comb created in 2000–2001 by using a femtosecond laser [21] is free from this disadvantage due to a high short-term stability of laser radiation, which allows the use of the laser as a 'flywheel' averaging the rapid phase noise of a radiofrequency generator.

In our experiment on the two-photon spectroscopy of hydrogen by using a semiconductor laser [7], the laser radiation frequency is doubled in two stages and then the 243-nm radiation is used to excite the 1s–2s transition in the hydrogen atom. This process involves eight laser photons, and the parameter η' is equal to η^{64}.

To study the validity of expression (8) in the optical range, we compared the spectra of beat signals between radiations from the stabilised dye laser and semiconductor laser at 486 and 243 nm, respectively (see Fig. 5). The data presented in Fig. 7a show that power fraction η in the carrier decreases after frequency doubling. We believe that the pedestal is related only to fluctuations of the semiconductor laser radiation because the dye laser radiation is characterised by phase fluctuations with longer correlation times, which are mainly caused by acoustic vibrations in the dye jet and vibrations of the laser cavity mirrors. In addition, we found that the phase noise level can be varied in a broad range by controlling the parameters of the

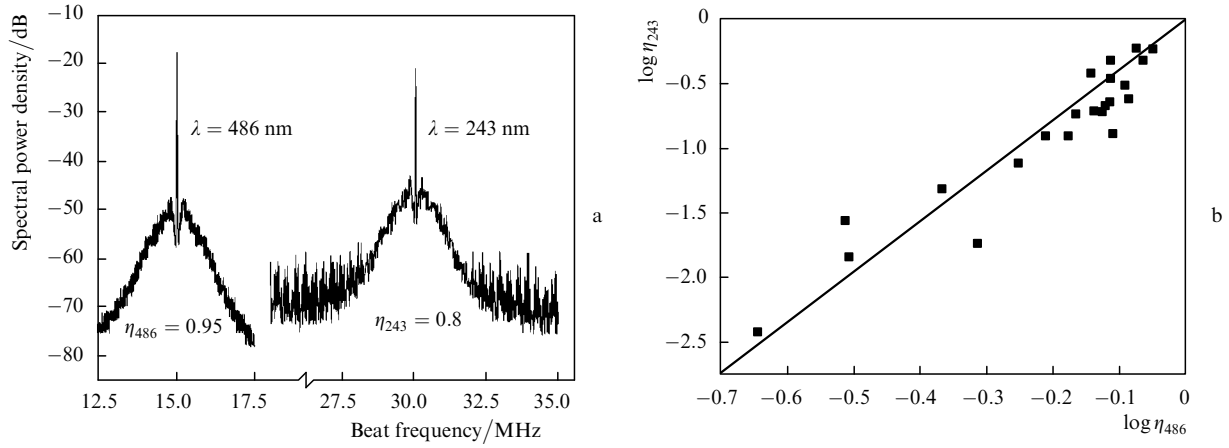

Figure 7. Spectral power density of the beat signal of radiation from the dye laser and semiconductor laser stabilised with respect to cavity 3 at wavelengths 486 and 243 nm (a) and the power fraction η_{243} contained in the carrier at a wavelength of 243 nm as a function of the power density η_{486} contained in the carrier at a wavelength of 486 nm (b).

feedback loop for the semiconductor laser by the PDH method (for example, the amplification or time constants of integrators). No changes in the spectrum with changing the parameters of the PDH stabilisation system of the dye laser were observed. By selecting feedback parameters, we managed to achieve the maximum value $\eta_{486} = 0.95$ for the second harmonic of the semiconductor laser, which approximately corresponds to $\eta_{972} = 0.99$ at the fundamental wavelength 972 nm or to the phase noise level $\phi_{\rm rms} = 6^\circ$. Figure 7b shows the mutual change in the power fraction contained in the carrier at wavelengths 486 and 243 nm with changing amplification in the feedback loop of the PDH stabilisation system of the diode laser. The slope of the fitting straight line is 3.9 ± 0.2, in good agreement with expression (8).

6. Spectral width of the carrier

The carrier has also the spectral width, which is mainly determined by fluctuations of the distance between reference cavity mirrors. Because the general theory of the spectrum of an oscillation with a randomly fluctuating frequency is quite complicated, we consider only two limiting cases of this theory [22].

Consider the electromagnetic oscillation of the field

$$E(t) = E_0 \cos\left(\omega_0 t + \int \Omega(t)\mathrm{d}t\right).$$

We assume that the distribution of the fluctuating part of the frequency $\Omega(t)$ is described by the normal law

$$p_\Omega(\Omega) = \frac{1}{\sqrt{2\pi}\Omega_{\rm rms}} \exp\left(-\frac{\Omega^2}{2\Omega_{\rm rms}^2}\right)$$

with the distribution width $\Omega_{\rm rms}$ and its average is zero, $\langle\Omega(t)\rangle = 0$. For simplicity, we assume that the frequency noise spectrum is white.

The first case under study corresponds to large correlation times τ_Ω for which $\Omega_{\rm rms}\tau_\Omega \gg 1$. The autocorrelation function of this process is

$$R_E(\tau) = \frac{1}{2}\cos(\omega_0\tau)\left\langle \cos\int_t^{t+\tau} \Omega(t)\mathrm{d}t\right\rangle \approx$$

$$\approx \frac{1}{2}\cos(\omega_0\tau)\int_{-\infty}^{+\infty} \cos(\Omega\tau)p_\Omega(\Omega)\mathrm{d}\Omega. \qquad (9)$$

This gives the spectral power density of the process:

$$g_E(\omega) = \frac{E_0^2}{\sqrt{8\pi}\Omega_{\rm rms}} \exp\left[-\frac{(\omega-\omega_0)^2}{2\Omega_{\rm rms}^2}\right]. \qquad (10)$$

Thus, $g_E(\omega)$ repeats the normal distribution of the frequency noise. When the radiation frequency is multiplied by n, the width of the spectrum also increases by n times.

The second case under study corresponds to small correlation times for which $\Omega_{\rm rms}\tau_\Omega \ll 1$. In this case, the model of phase diffusion with the diffusion coefficient $D = \frac{\pi}{2}g_\Omega$ can be applied, where g_Ω is the spectral power density of the frequency noise $\Omega(t)$ [22]. The spectral power density of the signal noise with phase diffusion is well known:

$$g_E(\omega) = \frac{E_0^2}{2\pi}\frac{D}{D^2 + (\omega-\omega_0)^2}. \qquad (11)$$

The multiplication of the frequency of this process by n leads to the multiplication of the spectral power density of the frequency noise by n^2 and, therefore, the width of the spectrum also increases by n^2 times.

Here a remark needs to be made concerning the possible high-frequency phase noise of the signal. It is accepted that the linewidth of stabilised lasers is the spectral width of their carrier. However, if the carrier disappears after multiphoton frequency conversion ('carrier collapse'), this definition of the laser linewidth becomes incorrect. In this case, it will be more appropriate to consider the spectral width of the pedestal, which can be greater than the initial width of the carrier by many orders of magnitude.

Thus, depending on the relation between the frequency noise level and the noise correlation time, the change in the spectral width of the central emission maximum of a stabilised laser after frequency multiplication can be substantially different. If the laser linewidth is determined by low-frequency acoustic vibrations or temperature drifts of the reference cavity, the laser line can be described by a Gaussian (10). In the case of fluctuations with a small correlation time, the shape of the carrier can be described by a Lorentzian (11).

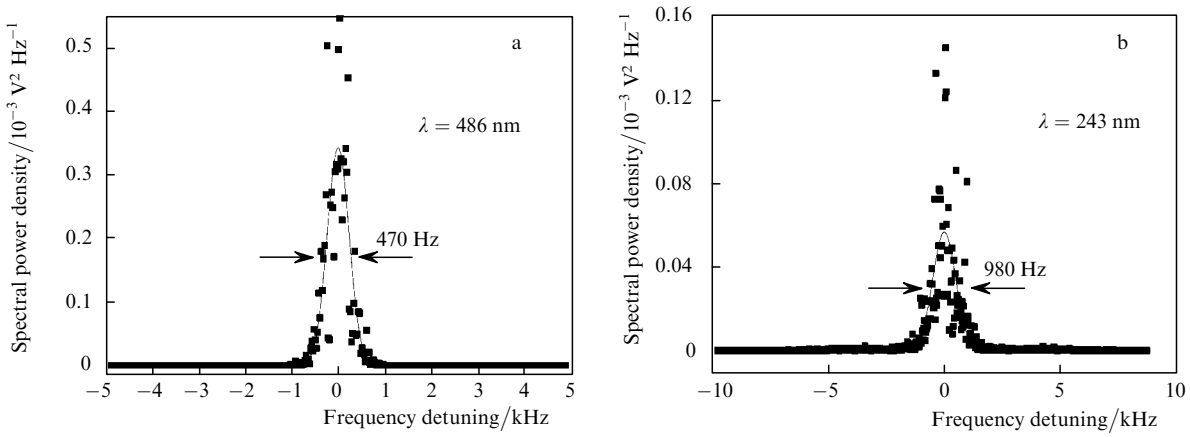

Figure 8. Spectral profiles of the beat signal carrier for radiations from the stabilised dye laser and the second harmonic of the semiconductor laser stabilised with respect to horizontal-axis cavity 1 (a) and after frequency doubling (b). Squares are experimental data, curves are approximation by Gaussians.

We studied the emission spectra of the semiconductor laser stabilised with respect to cavities 1 and 3 (Fig. 3), which considerably differ in their sensitivity to vibrations. Beat signals between radiations from the reference laser and laser under study at 486 and 243 nm (Fig. 5) were mixed with signals from a radiofrequency generator (with frequency lowering to a few hundreds of hertz) and studied with the help of a Fourier spectrum analyser.

Figure 8 shows the spectra of beat signals observed upon stabilisation of the semiconductor laser with respect to horizontal-axis cavity 1. The cavity was poorly isolated from mechanical vibrations, which explains large linewidths (spectra were recorded without averaging). The spectrum in Fig. 8a is well approximated by a Gaussian of width 470 ± 20 Hz. The profile of the beat signal at the doubled frequency (at 243 nm) has the width 980 ± 30 Hz. This means that the laser line is mainly broadened in this case due to acoustic vibrations of the cavity having large correlation times. Note that the contribution of the linewidth of the reference dye laser to the observed linewidth can be neglected.

Figure 9 presents similar spectra obtained upon stabilisation of the semiconductor laser with respect to cavity 3 (each spectrum was averaged over 20 realisations). Due to a low sensitivity of the vertical construction to vibrations (see below), the contribution of the linewidth of the semiconductor laser to the observed linewidth is negligible in this case. The beat signal is described by a Lorentzian of width 6.1 ± 0.1 Hz. After frequency doubling, the linewidth broadens by a factor of four up to 25.1 ± 0.1 Hz, in accordance with analysis performed above. Most likely noises with a small correlation time such as the laser intensity noise and noises of electronic elements play an important role in this case.

7. Characteristics of vertical-axis cavities

The spectral characteristics of the semiconductor laser stabilised with respect to the vertical-axis cavity were studied by using the scheme in Fig. 6 with equivalent cavities 3 and 4. The beat signal measured in these experiments is presented in Fig. 10a (averaging was performed over 14 realisations and the recording time was 8 s). The signal profile is described by a Lorentzian with a FWHM as small as 0.45 Hz, which satisfies most

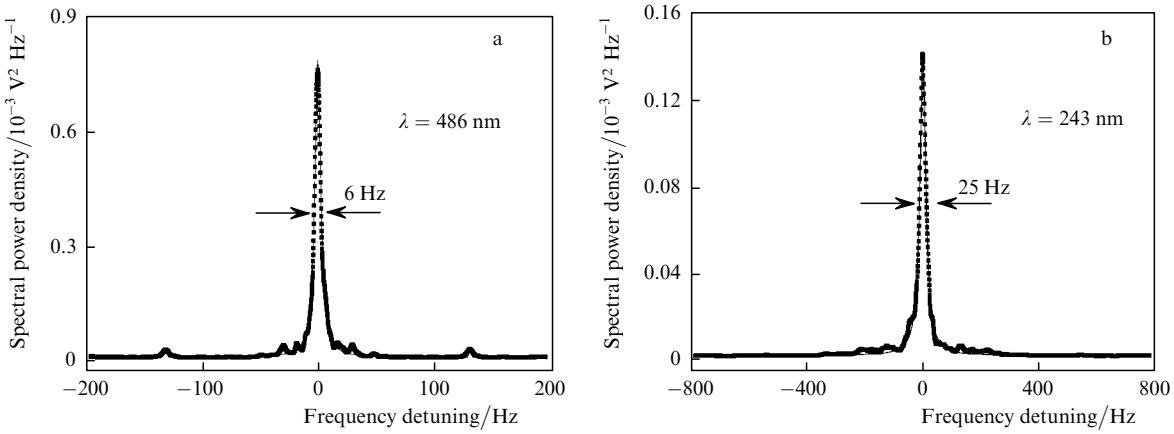

Figure 9. Spectral profiles of the beat signal carrier for radiations from the stabilised dye laser and the second harmonic of the semiconductor laser stabilised with respect to horizontal-axis cavity 1 (a) and after frequency doubling (b). Squares are experimental data, curves are approximation by Gaussians.

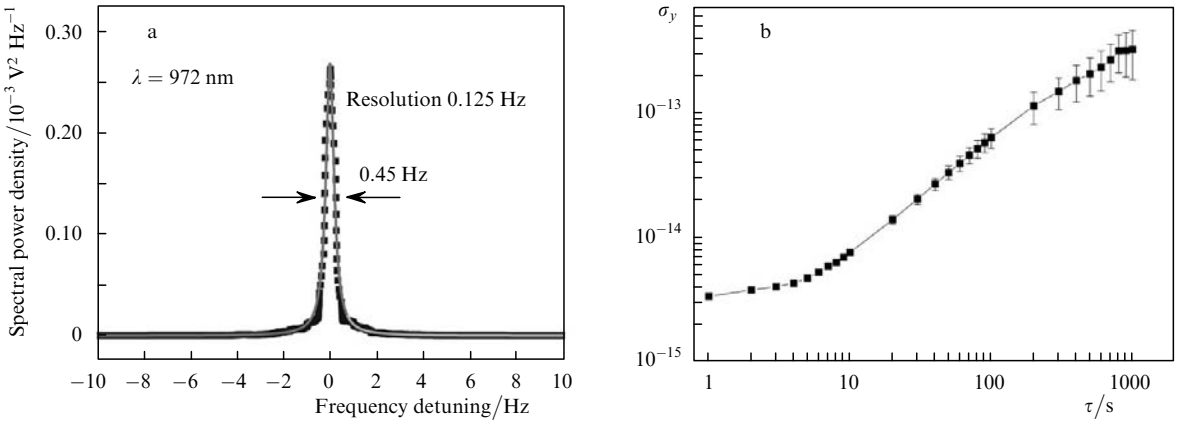

Figure 10. Spectrum of the beat signal between two light fields locked to cavities 3 and 4 (scheme in Fig. 6) recorded with a Fourier spectrum analyser with a resolution of 0.125 Hz (a) and the dependence of the Allan deviation σ_y on the averaging time τ for the beat signal of these fields, normalised to the light field frequency (b).

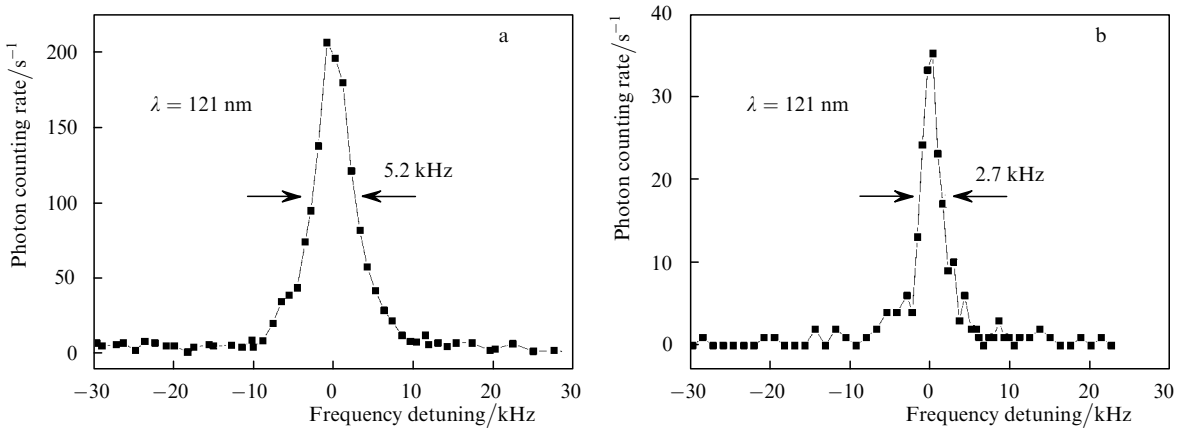

Figure 11. Spectra of the 1s–2s transition in the hydrogen atom recorded with the diode laser system stabilised with respect to cavities 1 (a) and 3 (b).

rigid requirements imposed on laser systems used in precision spectroscopy and atomic clock.

By measuring the frequency of the beat signal with a frequency counter, we constructed the Allan deviation plot (Fig. 10b) [23]. One can see that the relative instability of the system does not exceed 10^{-14} for the averaging time up to 100 s and then begins to increase due to temperature drifts.

We performed a number of measurements of the 1s–2s transition in the hydrogen atom by using the laser systems described above. The spectrum of the 1s–2s transition in the hydrogen atom (the Ly_α emission line of the hydrogen atom) (Fig. 11a) was recorded by using the semiconductor laser stabilised with respect to horizontal-axis cavity 1. The spectrum was obtained for an atomic hydrogen beam cooled down to 5 K; in this case, the detection scheme recorded signals only from atoms at velocities less than 150 m s^{-1}. By using the same laser system but stabilised with respect to vertical-axis cavity 3, we recorded the spectrum of the 1s–2s transition under similar experimental conditions (Fig. 11b). A considerable narrowing of the spectrum is explained by the better characteristics of the new reference cavity with the vertical axis. These experiments have shown that our laser system can be used for recording spectral lines of width ~1 kHz at 121 nm.

A comparison of the spectra obtained with the help of the semiconductor laser system (Fig. 11) with the spectra recorded by using the dye laser showed that excitation in the former case was less efficient approximately by 60 % [7]. Indeed, according to Eqn (8), $\eta_{121} = \eta_{972}^{64} = 0.99^{64} = 0.44$, in accordance with the experimental result.

8. Conclusions

We have studied the spectral characteristics of laser systems for spectroscopy of the 1s–2s transition in the hydrogen atom. The high-Q cavities of different configurations were manufactured and their sensitivity to temperature fluctuations and vibrations was analysed. The evolution of the shape of the emission spectrum after frequency doubling was studied and the power fraction in the carrier and the carrier width were determined.

It has been shown experimentally that the 972-nm semiconductor laser actively stabilised with respect to the vertical-axis cavity emits the line of width less than 0.45 Hz, the power fraction in the carrier being ~99 %. The laser instability does not exceed 10^{-14} at averaging times less than 10 s.

By using this laser system, we have recorded the spectra of the 1s–2s transition in the hydrogen atom and compared them with the spectra recorded by employing other stabilisation systems. It has been shown that the use of the vertical-axis cavity provides the considerable narrowing (down to 2 kHz) of the 1s–2s transition line of slow hydrogen atoms in a cold beam.

Acknowledgements. A.N. Matveev thanks V.N. Sorokin for stimulating discussions. This work was partially supported by the Alexander von Humboldt Foundation, the Foundation for Supporting the Russian Science, and the Russian Foundation for Basic Research (Grant No. 06-02-00443).

References

1. Rafac R.J., Young B.C., Beall J.A., Itano W.M., Wineland D.J., Bergquist J.C. *Phys. Rev. Lett.*, **85**, 2462 (2000).
2. Barber Z.W., Hoyt C.W., Oates C.W., Hollberg L., Taichenachev A.V., Yudin V.I. *Phys. Rev. Lett.*, **96**, 083002 (2006).
3. Ludlow A.D., Huang X., Notcutt M., Zanon-Willette T., Foreman S.M., Boyd M.M., Blatt S., Ye J. *Opt. Lett.*, **32**, 641 (2007).
4. Eichenseer M., von Zanthier J., Walther H. *Opt. Lett.*, **30**, 1662 (2005).
5. Niering M., Holzwarth R., Reichert J., Pokasov P., Udem Th., Weitz M., Hänsch T.W., Lemonde P., Santarelli G., Abgrall M., Lauren P., Salomon C., Clairon A. *Phys. Rev. Lett.*, **84**, 5496 (2000).
6. Fischer M., Kolachevsky N., Zimmermann M., Holzwarth R., Udem Th., Hänsch T.W., Abgrall M., Grunert J., Maksimovic I., Bize S., Marion H., Pereira Dos Santos F., Lemonde P., Santarelli G., Laurent P., Clairon A., Salomon C., Haas M., Jentschura U.D., Keitel C.H. *Phys. Rev. Lett.*, **92**, 230802 (2004).
7. Kolachevsky N., Alnis J., Bergeson S.D., Hänsch T.W. *Phys. Rev. A*, **73**, 021801 (2006).
8. Elliott D.S., Hamilton M.W., Arnett K., Smith S.J. *Phys. Rev. Lett.*, **53**, 439 (1984).
9. Notcutt M., Ma Long-Sheng, Ye Jun, Hall J.L. *Opt. Lett.*, **30**, 1815 (2005).
10. Young B.C., Cruz F.C., Itano W.M., Bergquist J.C. *Phys. Rev. Lett.*, **82**, 3799 (1999).
11. Drever R.W.P., Hall J.L., Kowalski F.V., Hough J., Ford G.M., Munley A.J., Ward H. *Appl. Phys.*, **31**, 97 (1983).
12. Riehle F. *Frequancy Standards* (WILEY-VCH Verlag GmbH Co. KGaA Weinheim, 2004).

13. Beverini N., Prevedelli M., Sorrentino F., Nyushkov B., Ruffini A. *Kvantovaya Elektron*., **34**, 559 (2004) [*Quantum Electron*., **34**, 559 (2004)].
14. Prevedelli M., Freegarde T., Hänsch T.W. *Appl. Phys. B*, **60**, 241 (1995).
15. Nazarova T., Riehle F., Sterr U. *Appl. Phys. B*, **83**, 531 (2006).
16. http://www.corning.com/specialtymaterials/.
17. Notcutt M., Ma Long-Sheng, Ludlow A.D., Foreman S.M., Ye Jun, Hall J.L. *Phys. Rev. A*, **73**, 031804R (2006).
18. Ma Long-Sheng, Jungner P., Ye Jun, Hall J.L. *Opt. Lett*., **19**, 1777 (1994).
19. Young B.C., Cruz F.C., Itano W.M., Bergquist J.C. *Phys. Rev. Lett*., **82**, 3799 (1999).
20. Telle H.R., in *Frequency Control of Semiconductor Lasers*. Ed. by M. Oshu (New York: Wiley, 1996) p. 137.
21. Udem Th., Holzwarth R., Haensch T.W. *Nature*, **416**, 233 (2002).
22. Rytov S.M. *Vvedenie v statisticheskuyu radiofiziku* (Introduction to Statistical Radiophysics) (Moscow: Nauka, 1976).
23. Allan D.W. *Proc. IEEE*, **54**, 221 (1966).